Article | Received 1 October 2024; Accepted 10 December 2024; Published 27 December 2024
https://doi.org/10.55092/exrna20240020

Impacting the gut microbiome through dietary plant-based extracellular vesicles

Hormat Rhein[1], Ardawna J. Green[1], Jian Yang[1], Melinda A. Engevik[2], Angela V. Serrano[3,4], Jessica K. Runge[3,4], Ruth Ann Luna[3,4], Sana Sharif[5], Xinli Liu[5], Kendal Hirschi[1,6] and Jennifer K. Spinler[3,4,*]

[1] Department of Pediatrics, Children's Nutrition Research Center, Baylor College of Medicine, Houston, Texas, USA
[2] Department of Regenerative Medicine & Cell Biology, Medical University of South Carolina, Charleston, SC, USA
[3] Department of Pathology & Immunology, Baylor College of Medicine, Houston, Texas, USA
[4] Texas Children's Microbiome Center, Department of Pathology, Texas Children's Hospital, Houston, Texas, USA
[5] Department of Pharmacological and Pharmaceutical Sciences, University of Houston, Houston, Texas, USA
[6] Department of Biological Sciences, The University of Texas at El Paso, El Paso, Texas, USA

* Correspondence author; Email: spinler@bcm.edu.

Abstract: Plant-based diets promote greater diversity and even distribution of gut microbiota which is beneficial to intestinal health, yet dietary complexity has hampered the ability to establish how specific components within a diet alter microbiome structure and function. Increasing evidence demonstrates that extracellular vesicles (EVs) act as prominent vehicles for cell-to-cell communication and inter-organismal transmission of RNAs, protein, and/or lipids. Plant-derived EVs have been found to mediate transport of various proteins and miRNAs, but how the makeup and content of EVs differ among crops and if these differences impact bioactivity is unknown. We have characterized EVs from potato and spinach and demonstrated that plant-derived EVs influence microbial growth *in vitro*. Using combined Fluorescence Activated Cell Sorting, high-resolution imaging, and 16S rRNA gene sequencing we have demonstrated that EV-microbe complexes can be isolated from a healthy human-derived microbial community, visualized EV internalization by these microbes, and characterized the microbial genera associated with EVs. Additionally, we have shown that plant-derived EVs can drive specific microbial shifts when incubated with human-derived microbial communities. These results suggest that plant-derived EVs can specifically influence bacterial growth and impact the gut microbiota, potentially enhancing the nutritional

benefits of plant-based diets. This research deepens our understanding of plant-derived EVs in gut health and could lead to advancements in plant-based nutritional therapies and drug delivery systems.

Keywords: plant diet; extracellular vesicles; plant-derived extracellular vesicles; *Lactobacillus*; *Lachnospiraceae*; gut microbiome; cross-kingdom communication

1. Introduction

Plant-based diets promote microbial diversity and stability in the gut which in turn promotes intestinal health [1]. While some aspects of these benefits are understood, the exact mechanisms through which plant-based diets exert their positive effects remain largely unknown. Research suggests that lipid-bound extracellular vesicles (EVs) derived from edible plants (EPDEVs) might play a role in these health benefits, acting as nanoparticles that contribute to the favorable properties of plant-based foods [2,3]. Plant EVs resemble those produced by mammalian cells [4] and have been shown to carry enzymes required for cell wall composition [5] that support a role in physiological processes like cell growth [6]. Plants also respond to pathogens using EVs to carry antimicrobial proteins and bioactive lipids that defend against fungal and bacterial pathogens [7–10]. Furthermore, plant-derived EVs are known to communicate across kingdoms through the transfer of small non-coding RNAs that may influence cell proliferation or virulence by silencing microbial genes through RNA interference [6,11–13]. All of this points to EPDEVs having the potential to impact human hosts through the gut microbiome.

Dietary advice often focuses on eating a variety of plant-based foods to ensure adequacy of an array of bioactive compounds [14]. However, the scientific underpinnings promoting this concept are inadequate [15], and the relationship between diet, microbiome, and consumer health is opaque. Research indicates that EPDEVs can endure the restrictive GI tract environment and protect the bioactive contents from inactivation or degradation [16]. Preserved bioactivity during transport supports that EPDEVs can influence gut microbiota, modulate immune responses, and provide antioxidant and anti-inflammatory benefits [13,16]. Research supports the model that EVs are species-specific and have the potential to differentially modulate gut bacteria [17]. Knowledge gained here will provide insights to understand how plant diets impact intestinal health and develop plant-derived EVs as a next generation drug delivery system or nutritional therapeutics.

In this study, we examined interactions of plant-derived EVs on the beneficial microbe *Lacticaseibacillus rhamnosus* GG (formerly *Lactobacillus rhamnosus* GG; LGG) and within healthy human-derived gut microbial communities. By combining fluorescence activated cell sorting, high-resolution imaging, and 16S rRNA gene sequencing, we examined EPDEV-microbe complexes within microbial communities, visualized the internalization of EPDEVs by these microbes, and characterized changes in microbial community structure associated with the presence of EPDEVs, while also assessing how the presence of plant-derived EVs impact microbial growth. This work starts to unravel the relationship between EPDEVs and gut microbiome modulation that could impact consumer health.

2. Methods

2.1. Plants and growth conditions

Potato and spinach lines were cultivated in a controlled greenhouse over the course of one year in an environment to try and ensure consistency and accuracy in growth assessment. The greenhouse located in Houston, TX, USA, maintained a temperature range of 22–24 °C during daylight hours and 20–22 °C at night. Relative humidity was not controlled, and supplementary artificial lighting was provided to ensure 12–16 hours of light daily. Plants were grown in well-drained soil, with regular irrigation to maintain consistent moisture levels, and systems were adjusted to try and prevent disease and optimize air circulation.

2.2. Isolation of plant-derived EVs

Extracellular vesicles were isolated from potato and spinach plants as previously described [18]. In brief, 50–60 day old potato leaves and 30 day old spinach leaves were harvested and vesicles were isolated from the apoplastic washes [19]. Approximately 35–50 grams of leaf tissue were harvested and vacuum infiltrated with vesicle isolation buffer (20 mM MES, 2 mM $CaCl_2$, and 0.1 M NaCl, pH 6). Excess fluid was removed from infiltrated plants by blotting. Then plants were placed inside 30-mL syringes within 50-mL conical tubes and centrifuged for 20 min at 700 × g and 4 °C (JA-14 rotor, Avanti J-20 XP centrifuge; Beckman Coulter). Apoplastic washes were 0.22-µm filtered and successively centrifuged at 4 °C for 1) 30 min at 10,000 × g and 2) 60 min at 40,000 × g. The vesicle pellet was resuspended in sterile Tris-HCl buffer (10 mM, pH 7.5) and stored at 4 °C until further use.

2.3. Characterization of plant-derived EVs

The hydrodynamic radius, polydispersity index (PDI), and zeta potential of the EVs were measured by dynamic light scattering (DLS) and electrophoretic light scattering techniques using a Litesizer DLS 500 (Anton Paar, Austria) device equipped with laser diode source at 658 nm and Kalliope software version 2.10.4. The DLS measurement for particle size was performed using the diluted EVs (1:20 fold) in Millipore water in a disposable cuvette at 90° scattering angle at 25 °C. The Stokes-Einstein equation [20] was used to obtain the particle diameter. Zeta potential was measured using the diluted EVs (1:20 fold) in Millipore water in an omega cuvette at 25 °C. Electrophoretic mobility values were recorded and Smoluchowski equation [21] was used to convert them to zeta potentials.

Nanoparticle tracking analysis (NTA) measurement was carried out to determine the size distribution and concentration of the EVs using a NanoSight LM14 instrument (Malvern, Westborough, MA, USA). The particle suspension was diluted 100-fold in Millipore water and injected into the laser module sample chamber with a 1-mL syringe at a syringe pump speed of 100 µL/min. The samples were illuminated by a laser light source at 532 nm and the flow of particles were monitored by an optical microscope. The capturing settings (camera

level of 16, gain of 1.5) were adjusted automatically and 30-second sample scanning recording at 30 frames/second were analyzed by using NTA3.4 software. Both systems were calibrated with 100 nm polystyrene beads (Nanosphere Size Standards, Thermo Scientific, Cat #3100A) diluted in Millipore water (1:100 fold) before each run. Between samples, the system was washed with Millipore water.

2.4. Bacterial strains, gut microbial communities, and culture conditions

Bacterial strains used in this study are listed in Table 1. Routine culturing of Lactic Acid Bacteria (LAB) in deMan, Rogosa, Sharpe medium (MRS; Difco, Franklin Lakes, NY, USA) was performed in an anaerobic chamber (Anaerobe Systems, AS-580, Morgan Hill, CA) supplied with a mixture of 10% CO_2, 5% H_2, and 85% N_2 for 16–18 h at 37 °C. Human-derived fecal microbial communities were incubated anaerobically in bioreactor medium (BRM2) [22]. Experiments requiring specific culture conditions are detailed individually.

Deidentified, filtered, frozen-thawed human-derived fecal preparations from healthy donors were obtained from the Texas Children's Microbiome Center. Working on ice, specimens were processed by 5 washes with 1X phosphate buffered saline (PBS) and filtering steps to remove residual fecal matter and retain microbial community members. Filtrates containing fecal microbial communities were stored in 15–20% glycerol at −80 °C until further use.

Table 1. List of bacterial strains used in this study.

Strain	Description	Source
***L. acidophilus* ATCC 4356**	Probiotic strain, human isolate	ATCC[a]
***L. casei* ATCC 334**	Probiotic strain isolated from Emmental cheese	ATCC
***L. reuteri* ATCC PTA 6475**	Probiotic strain, isolated from Finnish mother's milk	Biogaia AB
***L. reuteri* DSM 17938**	Daughter strain derived from *L. reuteri* ATCC 55730	Biogaia AB
***L. rhamnosus* GG**	Probiotic strain, human isolate	ATCC

[a]American Type Culture Collection (ATCC).

2.5. Effect of plant-derived EVs on the growth of lactobacilli

The effect of plant-derived EVs on the growth of various LAB was determined. Bacteria routinely cultured as described above were used to inoculate pre-reduced, fully-defined LDM4 medium [23] to an adjusted OD_{600} 0.05 with or without EVs (1.4×10^4 particles/µL). Working in an anaerobic chamber, cultures with and without EVs were aliquoted into a pre-reduced, sterile, flat-bottomed 96-well plate, and topped with 30 µL mineral oil. Plates were incubated at 37 °C for 18 h in a Synergy™ H1 Hybrid Multi-Mode Microplate Reader (BioTek Instruments, Inc, Winooski, VT, USA) where optical density measurements (600 nm) were recorded in 10-minute intervals. Results were compared to lactobacilli only (growth control),

and the maximum change in growth calculated. Significance was determined using student's *t*-test with equal variances.

2.6. Fluorescent labeling of LGG, human-derived fecal microbial community, and EVs

LGG or bacteria from a human-derived fecal microbial community were fluorescently labeled with carboxyfluorescein diacetate succinimidyl ester (CFDA-SE) as previously described [24] for downstream confocal microscopy and FACS studies. LGG was cultured anaerobically to exponential growth phase in MRS media and washed 2X in sterile anaerobic 1X PBS. The washed LGG or processed fecal microbial community was resuspended in anaerobic PBS and incubated at 37 °C anaerobically for 1 h with 10 µM CFDA-SE (Thermo Fisher, C1157). Cells were collected by centrifugation for 5 min at 5000 × g, then washed 3X in anaerobic PBS. Microscopy was used to confirm fluorescence.

Plant-derived EVs were labeled with a lipophilic dye per manufacturer's instructions for downstream confocal microscopy and FACS studies. EVs (7.01×10^7/mL) isolated and purified as described above, were brought up to 1 mL with diluent C, mixed with 6 µL of PKH26 dye (Sigma-Aldrich, MIDI26), and incubated for 5 min at room temperature. The labeling reaction was quenched with 2 mL 10% bovine serum albumin (BSA) and EVs re-collected by ultracentrifugation as described above. Labeled EVs were confirmed by microscopy and stored at −80 °C until further use [25].

2.7. EV uptake assay and analysis

Fluorescently labeled lactobacilli or human-derived fecal microbial community were co-incubated with fluorescently labeled EVs and assayed by confocal microscopy or FACS for EV uptake. In brief, CFDA-SE-labeled bacteria (5×10^7 cells/mL) were mixed with 3.5×10^6 PKH26-labeled EVs in either MRS for lactobacilli, BRM2 for fecal microbial communities, or 1X PBS for controls and incubated for 30 min on ice or at 37 °C. Cells were pelleted for 5 min at 8000 × g, then washed in 2X in PBS to remove free EVs, and finally filtered into 5 mL tubes with a 35 µM filter cap (VWR, catalog # 21008-948).

For analysis by fluorescent confocal microscopy, washed and filtered EV-uptake reactions containing LGG were spotted onto microscope slides, air-dried and cover slipped with mounting media. Slides were stored at RT in the dark until imaging. Slides were imaged using a Zeiss AxioVision with a 100X objective.

EV-uptake reactions containing either LGG or human-derived fecal microbial community were also analyzed and sorted by fluorescence-activated cell sorting using a FACS Aria II (Becton Dickinson (BD)) with 70 µm/70 psi nozzle carried out by the Baylor College of Medicine cytometry and Cell Sorting Core. Imaging of sorted populations was carried out on an Amnis ImageStream instrument from Cytek Biosciences. Sorted cells were collected and stored at –80°C for downstream analysis by next generation sequencing.

2.8. Effect of plant-derived EVs on fecal microbial community

The effects of plant-derived EVs on human-derived fecal microbial communities were assessed in static 24 h anaerobic cultures. Replicate reactions (eighteen independent 10 mL reactions in 50-mL conical tubes) were prepared in BRM2 [22] and conducted in an anaerobic chamber with a gas composition of 5% H_2, 5% CO_2, 90% N_2. Each reaction was inoculated with an anaerobic preparation of a 15% w/v fecal microbial community slurry to a final concentration of 3.75% fecal microbial community. After 16 h of outgrowth, nine reactions were treated with 4×10^{10} plant-derived EVs per µL, and nine reactions treated with buffer. Samples (1 mL) were collected from each 10 mL reaction at 0 and 24 h post inoculation with EVs or buffer, centrifuged for 1 min at 21,000 × g, and pellets stored at −80°C until 16S rRNA gene sequencing was performed as described below.

2.9. 16S rRNA gene sequencing and data processing

Extraction and 16S rRNA gene sequencing of microbial DNA were carried out as described by the Human Microbiome project [26]. Briefly, microbial pellets were processed through the Qiagen DNeasy UltraClean Microbial kit protocol, formerly MoBio Laboratories UltraClean® Microbial DNA Isolation Kit, using a reduced elution volume. DNA was quantitated using the high-sensitivity dsDNA assay kit on a Qubit® 2.0 fluorometer (Thermo Fisher Scientific, Inc.). DNA samples were stored at −20 °C until further processing.

Amplification of the V4 region of the 16S rRNA gene (20 ng input DNA) was performed with the NEXTFlex® V4 Amplicon-Seq Kit 2.0 (Bioo Scientific), as previously described [27]. Paired-end sequencing (2 × 250 bp) of pooled 16S libraries was performed on an Illumina MiSeq® instrument (Illumina) following the standard Illumina sequencing protocol using a 500-cycle v2 chemistry kit [28].

16S rDNA gene sequences (v4 region) were demultiplexed and denoised using the DADA2 [29] algorithm incorporated in QIIME2 version 2023.5. Taxonomic assignment of previously defined amplicon sequence variants (ASVs) was performed using the feature classifier *classify-sklearn* and the SILVA database, (version 13.8.1) [30,31] with a p-confident value of 0.8. Taxa not classified at the phylum level or classified as chloroplasts or mitochondria were excluded from analysis. Representative sequences (ASVs) were aligned with MAFFT [32] and both an unrooted and rooted trees were calculated with FASTTREE [33] to generate phylogenetic diversity metrics. Visualization and statistical analyses of bacterial community diversity and composition of ASVs were evaluated using MicrobiomeAnalyst 2.0 [34] and STAMP [35] packages. The Mann-Whitney U test was used to determine significant differences in alpha diversity, while beta diversity of non-rarefied taxon data was explored with Jensen-Shannon divergence and PERMANOVA. Taxon specific abundance between treatment groups (before EVs, 24h post EVs, 24h no EVs) was evaluated using STAMP and significance determined with White's non-parametric t-test with a $p\text{-value} < 0.05$.

3. Results

3.1. Potato-derived EVs are internalized by LGG

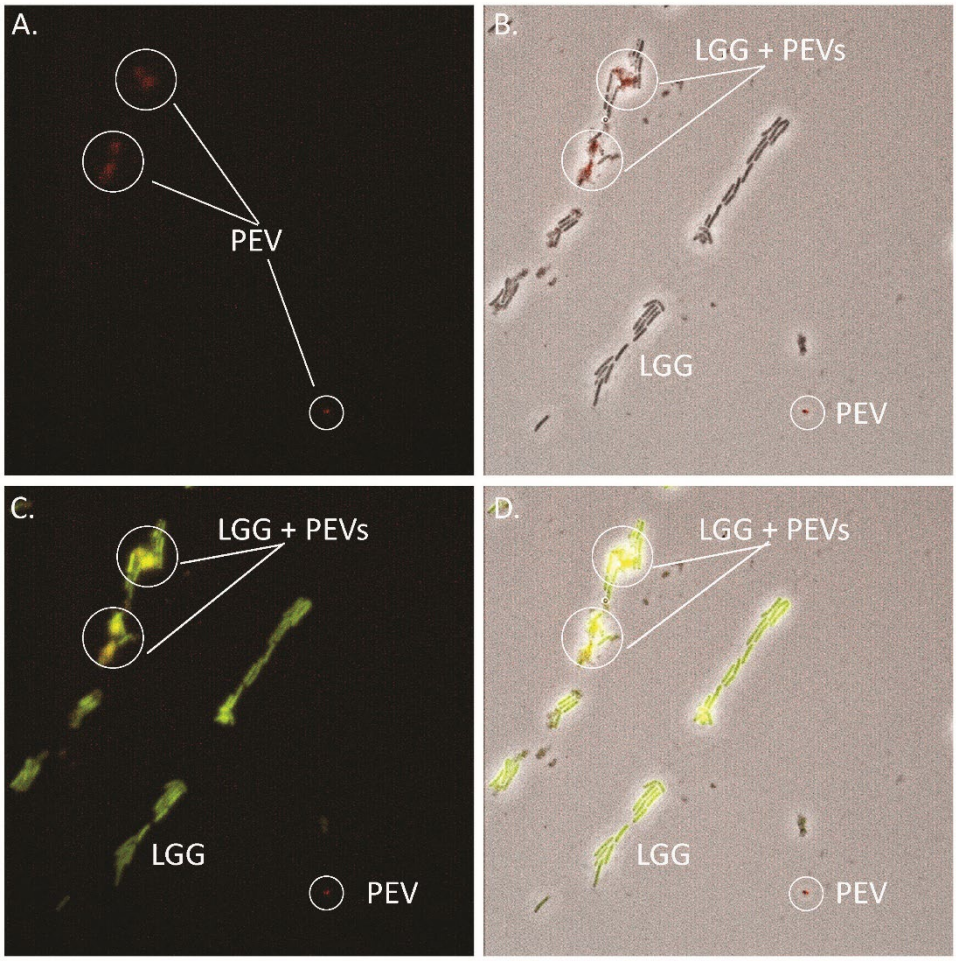

Figure 1. Co-localization of potato-derived extracellular vesicles and LGG. Representative images of reactions containing PKH26-labeled PEVs (red) and CFDA-SE-labeled LGG (green). PEVs are seen in red under (**A**) dark-field fluorescent imaging and (**B**) fluorescent imaging coupled with phase contrast. LGG (green) are seen in the presence of PEVs (red fluorescence) with overlapping LGG and PEVs in yellow fluorescence in dark-field (**C**) and with phase contrast (**D**). Images were produced with a Zeiss Axiovision using a 100X objective.

Previous work has shown EVs isolated from edible plants like ginger, tomato, and garlic are taken up by lactobacilli and influence the growth and composition of beneficial microbes and other gut microbiota [36–39]. Specifically, Teng *et al.* has shown plant-derived EVs to be preferentially taken up by LGG [36], which is one of the most studied probiotics in humans [40]. The safe use of LGG has been demonstrated in a variety of patient populations that include pregnant women, premature neonates, the elderly, and others with underlying health conditions [41]. Also, LGG is protective against intestinal infections associated with viruses [42–44] and antibiotics [45–47], and is also known to positively impact inflammatory

diseases like atopic dermatitis [48,49]. Here we used microscopic imaging and fluorescence assisted cell sorting (FACS) techniques to test the hypothesis that EVs isolated from potato could be internalized by probiotic LGG. Potato EVs (PEVs) were isolated and characterized by direct light scattering (DLS) and nanoparticle tracking analysis (NTA) to estimate their hydrodynamic diameter and concentration, respectively. The average diameter and concentration of isolated PEVs was 244 nm at $7.01 \times 10^7 \pm 3.28 \times 10^6$ particles/mL (Figure S1). The particle size polydispersity index and zeta potential of PEVs were 0.24 and -15.4 mV, respectively. PEVs (7.01×10^5) were labeled with PKH26 (red), incubated with 1×10^7 CFDA-SE-labeled LGG (green) and analyzed by fluorescent microscopy to visualize co-localization of PEVs and LGG. Fluorescent microscopic imaging at 100X (Figure 1) showed evidence of PEVs co-localizing with LGG but could not resolve internalization at this resolution.

To further investigate if PEVs were internalized by LGG, we used FACS analysis combined with high-content image analysis to isolate, quantify, and visualize PEV-LGG complexes. To ensure we could use FACS to sort LGG, PEVs, and PEV-LGG complexes, we tested mixtures of CFDA-SE-labeled or unlabeled LGG (5×10^7 cells) with and without PKH26-labeled or unlabeled PEVs (3.5×10^6) as summarized in Table 2. We also tested the effect of media and temperature on PEV uptake by LGG (Table 2). Using a BD FACSAria II Cell Sorter we sorted and quantified PKH26-labeled PEVs, CFDA-SE-labeled LGG, and labeled PEV-LGG complexes from each condition. In Figure 2A, we show that FACS can quantify and differentiate between fluorescently labeled LGG, PEVs, and PEV-LGG populations containing both fluorescent labels (co-localization). Control reactions containing only CFDA-SE-labeled LGG showed that when sorting for 10,000 CFDA-SE-labeled (green) events (Figure 2B, panel LGG), expectedly no PKH26-labeled (red) events were captured. Similarly, when 10,000 PKH26-labeled (red) events were sorted from a control reaction containing only PKH26-labeled PEVs, a very small proportion (0.13%) of events were counted as CFDA-SE-labeled events (Figure 2B, panel PEVs). Quantification of ~50,000 sorted events from each uptake reaction (UR, Table 2) that contained both CFDA-SE labeled LGG and PKH26-labeled PEVs showed that co-incubation of LGG with PEVs at 37°C in a rich nutrient source (MRS) resulted in a 3.2-fold increase in sorted PEV-LGG complexes when compared to a nutrient deplete source (PBS) at 37°C (Figure 2B, panel PEV-LGG). Sorted populations of PEV-LGG dual-labeled events increased 1.6-fold when incubated in a nutrient rich source at 37 °C compared to 4 °C (Figure 2B, panel PEV-LGG) indicating the biologically relevant temperature is important for PEV uptake by LGG. Sorting of PEV-LGG complexes increased by 3.6-fold when incubated in a nutrient rich media compared to PBS at 4 °C, further indicating the importance of a rich medium for uptake at either temperature (Figure 2B, panel PEV-LGG). Further flow cytometry-based high-content image analysis using the Amnis ImageStream instrument indicated that the dual-fluorescent PEV-LGG population represents PEV internalization by LGG. Representative images of single-fluorescent populations (LGG or PEVs) and dual-fluorescent populations (PEV-LGG) are depicted in Figure 2C. For Figure 2C, channel 01 (Ch01) shows brightfield images of sorted LGG bacteria, while channels 02 and 03 (Ch02, Ch03) show fluorescent images of CFDA-

SE-labeled LGG and PKH26-labeled PEVs in the same field, respectively. When Ch01 and Ch03 are overlain, we observe that the PKH26-labeled entities take the shape of the bacteria. Implications of these data are that LGG does internalize PEVs and optimally requires a nutrient rich media and a biologically relevant temperature.

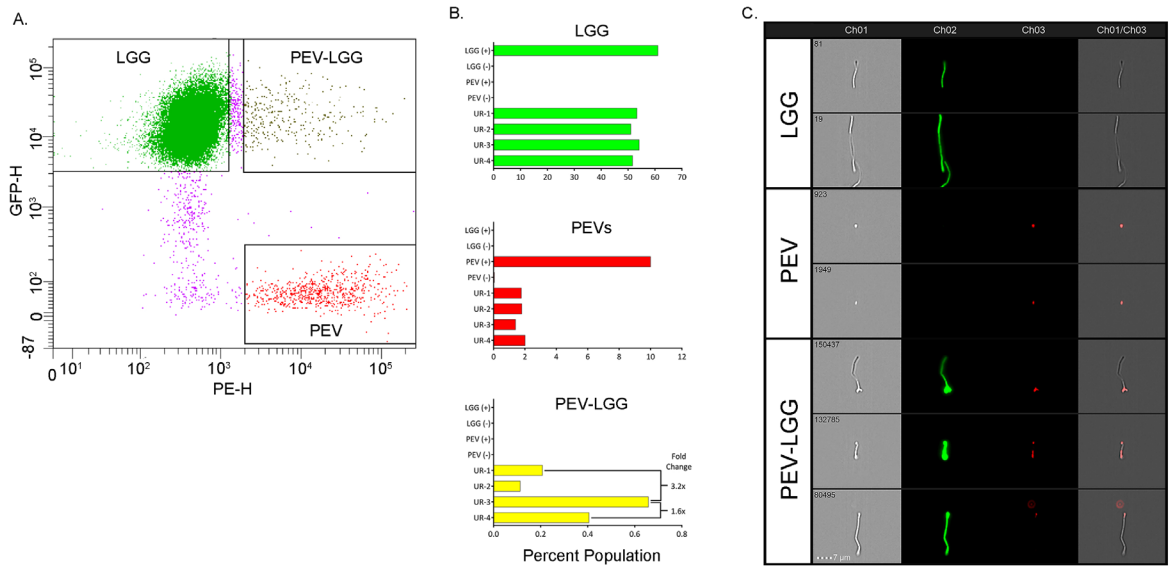

Figure 2. FACS analysis and high-resolution imaging verifies LGG uptake of potato-derived EVs. (**A**) Scatter plot of fluorescent events show the separation of LGG = fluorescent green events, PEV = red fluorescent events, and PEV-LGG = dual green-red fluorescent events. (**B**) Quantitation of sorted events with a single fluorescent green label (LGG; green bars), single fluorescent red label (PEVs; red bars), or dual fluorescent green and red labels (PEV-LGG; yellow bars) are represented in corresponding bar graphs. Fold change between uptake reactions (UR) is indicated on the PEV-LGG bar graph. (**C**) Images produced by Amnis ImageStream analysis shown represent populations sorted for LGG, PEVs, and PEV-LGG. Ch01 = channel 01, brightfield microscopy; Ch02 = channel 02, green fluorescence; Ch03 = channel 03, red fluorescence; Ch01/Ch03 = brightfield microscopy overlain with red fluorescence.

Table 2. Summary of uptake reactions tested by FACS.

Sample	Label	LGG (cells)	PEVs (μL)	Time (min)	Temp (°C)	Buffer/Media
LGG (+)	CFDA-SE	5×10^7	0	30	Ice	PBS
LGG (-)	None	5×10^7	0	30	Ice	PBS
PEV[a] (+)	PKH26	0	50	30	Ice	PBS
PEV (-)	None	0	50	30	Ice	PBS

Table 2. *Cont.*

Sample	Label	LGG (cells)	PEVs (µL)	Time (min)	Temp (°C)	Buffer/Media
UR[b]-1	CFDA-SE/PKH26	5×10^7	50	30	37	PBS
UR-2	CFDA-SE/PKH26	5×10^7	50	30	Ice	PBS
UR-3	CFDA-SE/PKH26	5×10^7	50	30	37	MRS
UR-4	CFDA-SE/PKH26	5×10^7	50	30	Ice	MRS

[a]PEV = potato-derived extracelluar vesicle; [b]UR = uptake reaction.

3.2. Potato-derived EVs influence the growth of additional beneficial lactic acid bacteria

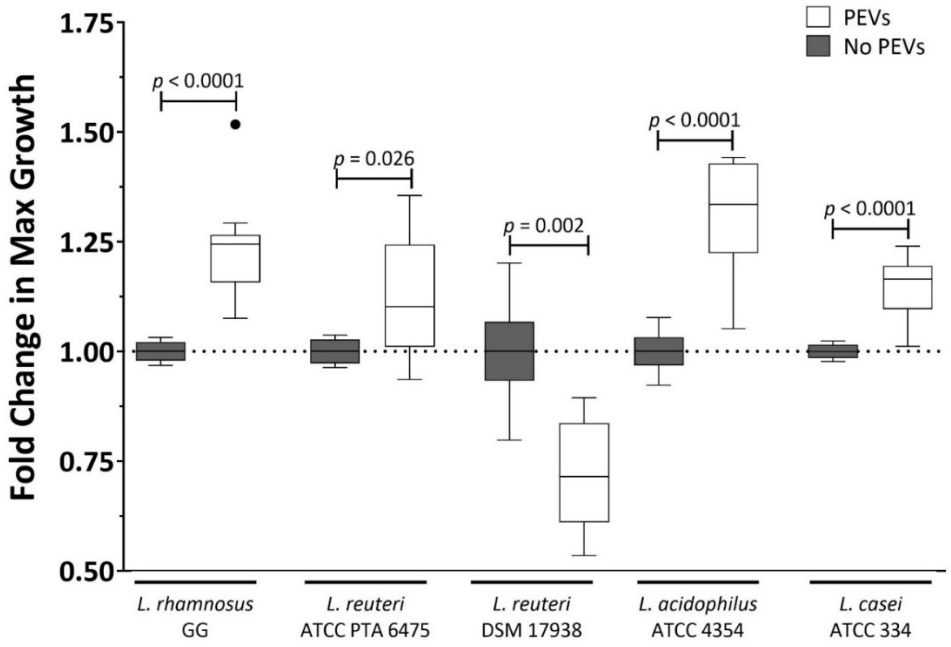

Figure 3. Potato-derived EVs differentially impact growth of beneficial lactobacilli. Five species of lactobacilli were cultured in the presence and absence of PEVs and growth measured by OD600 at 10-minute intervals for 18 h. Max growth in the presence and absence of PEVs was compared to media control and fold-change in max growth plotted per organism with (white bars) and without (gray bars) PEVs. Unpaired Welch's t-test was used to calculate significance.

To determine the potential for PEV-mediated growth effects on gut microbes, we incubated PEVs with different lactobacilli and measured anaerobic growth in 10 min intervals at 37 °C over 18 h. Growth curve data were plotted, analyzed, and showed species-specific growth effects among five different species of lactobacilli: LGG, *Limosilactobacillus reuteri* ATCC PTA 6475, *L. reuteri* DSM 17938, *Lactobacillus acidophilus* ATCC 4354, and *Lacticaseibacillus casei* ATCC 334 (Figure S2). Fold change in max growth as measured by OD600 was determined per strain relative to media control and showed that PEVs positively

impacted growth at varying degrees for LGG, *L. reuteri* ATCC PTA 6475, *L. acidophilus* ATCC 4354, and *L. casei* ATCC 334, but negatively impacted growth of *L. reuteri* DSM 17938 (Figure 3, Figure S2). PEV-mediated growth effects were most pronounced for LGG (1.24-fold, $p < 0.0001$) and *L. acidophilus* ATCC 4354 (1.31-fold, $p < 0.0001$) (Figure 3). Interestingly, two strains of human-derived *L. reuteri* representing distinct clades of the species [50] responded differently to treatment with PEVs. *L. reuteri* ATCC PTA 6475 responded with a small but perceptible 1.2-fold increase in growth ($p < 0.05$) while *L. reuteri* DSM 17938 consistently responded with a decrease in growth over time (0.7-fold, $p < 0.01$) (Figure 3). Subsequently, PEVs were treated with RNase A or proteinase K and the PEV-mediated growth effects on LGG and *L. acidophilus* tested. Growth effects were independent of proteinase K or RNase A treatments and buffer controls had no impact on growth (data not shown). These different responses from various species and strains of lactobacilli show how EPDEVs can have specific influences over different organisms and highlight that their effects should not be generalized across bacterial genera or species, but instead dissected to better understand how these specific effects occur.

3.3. Potato-derived EVs interact with gut bacteria

PEVs were combined with a mixed bacterial community prepared from healthy human donor stool to determine if PEVs could be internalized by human-derived gut microbes other than lactobacilli using FACS combined with high-content image analysis. Based on the optimized conditions determined with LGG, six uptake reactions of CFDA-SE-labeled gut bacteria (5×10^7 cells) derived from healthy donor stool incubated with PKH26-labeled PEVs (3.5×10^6) in nutrient rich media (BRM2) at 37 °C were analyzed. Dual-fluorescent populations were sorted and imaged as done previously. Similarly to LGG, PEV internalization by various gut bacteria was observed and representative images are shown in Figure 4A. In Figure 4A, bacterial morphology is shown through bright field microscopy in Ch01, green fluorescent bacteria or red fluorescent PEVs of the same field of image are shown in Ch02 and Ch03, respectively. Ch01 and Ch03 are overlain (Ch01/Ch03) to visualize that the red fluorescence from PEVs takes the shape of the bacteria sorted, suggesting bacteria have internalized PEVs. Sorted dual-fluorescent populations were collected for downstream bacterial identification by 16S rDNA sequencing.

To identify what kinds of human-derived gut microbes were capable of internalizing PEVs, the DNA of collected populations of dual-fluorescent PEV-bacteria complexes was extracted and analyzed by 16S rRNA gene sequencing to identify the bacteria associated with PEV-internalization. The sunburst plot in Figure 4B illustrates the distribution of taxa identified at the phylum, family, and genus levels. Percent relative abundance showed that over 78% of the dual-fluorescent sorted population represented organisms from the phylum Firmicutes, with others belonging to phyla Bacteroidota (16.1%) and Actinobacteriota (5.3%). Most of the organisms within the Firmicutes phyla belonged to the *Lachnospiraceae* family and included genera *Blautia* (36.7%), *Anaerostipes* (10.8%), *Agathobacter* (8.9%), and *Roseburia* (8%). Other Firmicutes included the genera *Faecalibacterium* (9.7%) and

Romboutsia (4.5%). *Bacteroides* spp. (16.1%) was the only genus representing the Bacteroidota phylum. Likewise, *Bifidobacterium* spp. (5.3%) solely represented the Actinobacteriota phylum.

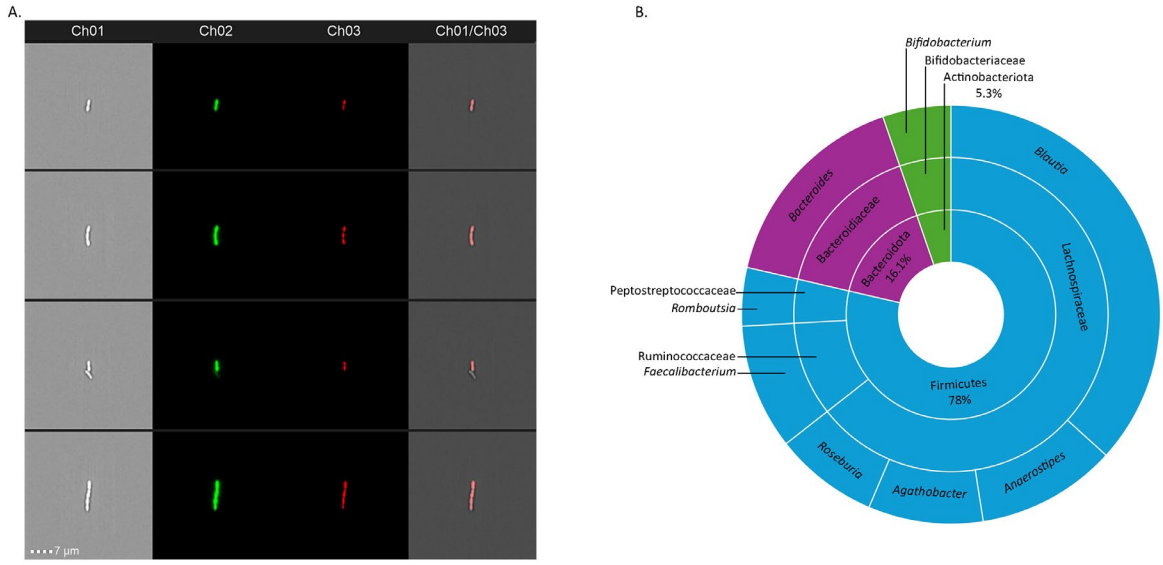

Figure 4. FACS analysis and 16S rRNA gene sequencing identify human-derived gut microbes associated with PEV uptake. CFDSE-labeled microbial communities were mixed with PKH26-labeled PEVs in BRM2 media and incubated at 37 °C to encourage uptake of PEVs by gut microbes. Cells were sorted based on fluorescence and images produced by Amnis ImageStream analysis shown (A) represent populations sorted for LGG, PEVs, and PEV-LGG. Ch01 = channel 01, brightfield microscopy; Ch02 = channel 02, green fluorescence; Ch03 = channel 03, red fluorescence; Ch01/Ch03 = brightfield microscopy overlain with red fluorescence. Sorted populations were analyzed by 16S rRNA gene sequencing to identify bacteria associated with PEV uptake. Identified bacteria are depicted in a sunburst diagram (B).

3.4. Plant-derived EVs associate with small changes in microbial composition of mixed gut communities

Having established that PEVs associate with specific organisms using FACS and 16S rRNA sequencing, we wanted to know if another type of EPDEV could impact a healthy human-derived gut microbial community. We isolated and tested the effects of EVs from the leafy vegetable spinach (SEVs) on human-derived gut microbial communities. SEVs were analyzed by DLS and NTA to estimate their hydrodynamic diameter and concentration, respectively. The average diameter and concentration of isolated SEVs was 308 nm with a concentration of $5.35 \times 10^{10} \pm 8.21 \times 10^{8}$ particles/mL (Figure S3). The particle size polydispersity index and zeta potential of SEVs were 0.23 and −41.4 mV, respectively. Mixed microbial communities derived from healthy human donor stool were used to model the effects of EPDEVs on human gut microbial communities in static anaerobic culture. First, microbial communities were established in anaerobic culture for 16 h prior to treatment with

SEVs, then established cultures (n = 18) were incubated with (n = 9, Spinach) and without (n = 9, Control) SEVs for 24 h. Samples of established communities for each group (Control and Spinach) were obtained after the initial 16 h incubation (prior to the addition of SEVs) to establish baseline microbial community structure (T0). Additional samples were taken for each group at 24 h (T24 Control, T24 Spinach) to assess the potential effects of SEVs on microbial community composition. We sequenced the V4 variable region of 16S rRNA genes in DNA isolated from these samples to determine 1) how the 24 h microbial communities evolved from baseline (T0), and 2) how communities treated with SEVs (T24 Spinach) differed from untreated (T24 Control) communities.

Longitudinal comparisons of 16S rRNA gene sequence data showed changes in microbial community structure from that of the established baseline communities (T0) after 24 h (T24 Control, T24 Spinach). Changes in beta-diversity were assessed using Jensen-Shannon divergence and visualized through principal coordinate analysis (PCoA) (Figure 5A). Statistical significance of community structure differences using PERMANOVA demonstrated that the differences between baseline communities (T0) and those present 24 h later for control (T24 Control) or SEV-treated samples (T24 Spinach) were substantial and significant (p = 0.001) with F-values of 756.05 and 782.23, respectively. PERMANOVA analysis indicated that the differences in microbial communities between control (T24 Control) and SEV-treated samples (T24 Spinach) were much smaller (F-value = 9.4602), however these small changes in community structure were significant with a *p-value* = 0.002. Chao1 and Observed alpha-diversity measures (Figure 5A) show a significant shift by ANOVA in the number of species between baseline (T0) and both T24 Control ($p < 0.0001$) and T24 Spinach groups ($p = 0.0014$), indicating that the anaerobic 24 h incubation decreased the number of different species present in each test group. However, ANOVA indicated no significant differences in the number of species (Chao1 or Observed) between T24 Control and T24 Spinach groups ($p = 1$). Shannon and Simpson alpha-diversity measures (Figure 5A) indicate the richness and evenness of the baseline community was greater than those at 24 h, respectively, while the richness and evenness of the T24 Control and T24 Spinach communities were relatively the same.

Comparisons of the ASV abundances between communities reflect what has been visualized with alpha- and beta-diversity measures in Figure 5. Shifts in the relative abundance at the genus taxonomic level can be seen between T0 and the T24 groups, while changes between T24 Control and T24 Spinach groups are more subtle (Figure 5B). We used the graphical software package STAMP (Statistical Analysis of Taxonomic and Functional Profiles) [35] to quantify the taxonomic differences between T24 Control and the SEV-treated group (T24 Spinach) and provide the details behind the small but significant differences identified through beta-diversity. Through STAMP, we identified significant genus-level taxonomic shifts between T24 Control and T24 Spinach groups and these taxa are represented in Figure 5C. Consistent with data shown using PEVs, we show that a human-derived gut microbial community treated with spinach-derived EVs primarily affected ASVs within the Firmicutes phyla and resulted in increases in *Lactobacillus* spp. and ASVs present in the *Lachnospiraceae* (Firmicutes phylum) and *Enterobacteriaceae* (Proteobacteria

phylum) families. Conversely, decreases in ASVs present in the *Butyricioccus* and *Blautia* genera were observed in the T24 Spinach group compared to T24 Control. These differences in taxa between T24 Control and T24 Spinach groups were deemed significant at *p-values* < 0.05 using the Welch's T-Test.

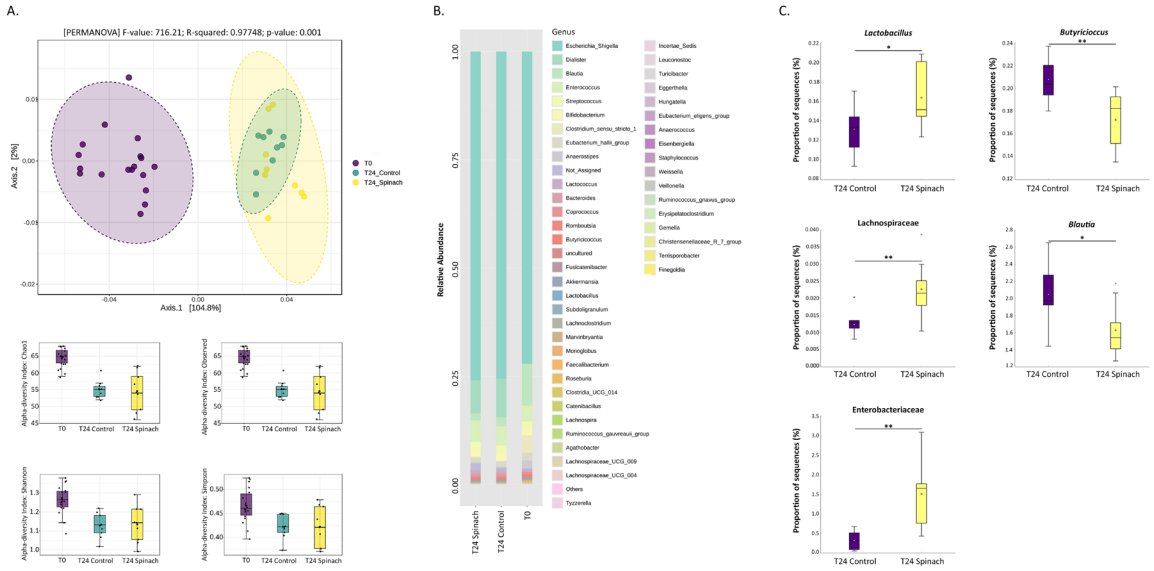

Figure 5. Plant-derived EVs influence the abundance of specific microbes in a complex community. Microbial community composition and structure was investigated temporally using 16S rRNA gene sequencing and is shown through (**A**) Jensen-Shannon divergence at the ASV level. Relative abundance of taxa at the genus level are shown in (**B**). Taxa with significant differences in abundance between T24 Control and T24 Spinach groups are represented in (**C**) box-and-whisker.

4. Discussion

Assessing the bioavailability and bioactivity of EVs derived from edible plants can be complex, especially when focusing on serum stability and their effects on tissues far from the site of dietary intake. A fundamental aspect of this research is that EPDEVs are primarily bioactive in the intestine, where their concentrations are highest. Additionally, these EPDEVs resemble mammalian EVs structurally and interact with soil microbiomes and plant pathogens which support their role in cross-kingdom communication, suggesting they play a broader role in the ecosystem [51,52]. Each plant contributes a unique profile of EPDEVs, which in theory could differentially affect the gut microbiome (Figure 6). Lactobacilli are common beneficial microbes that are either supplied by diet or are endogenous to the human gastrointestinal (GI) tract. Fermented food products containing lactobacilli have demonstrated efficacy in promoting digestive health. Previous studies have shown that EPDEVs isolated from ginger [36] and tomato [37] have effects on lactobacilli. Here we showed EPDEVs from two different plants, potato and spinach, also influence growth of lactobacilli whether in single-organism culture or a mixed microbial community. This

additional data supports the hypothesis that beneficial lactobacilli may have evolved to work synergistically with plant diets to benefit host health.

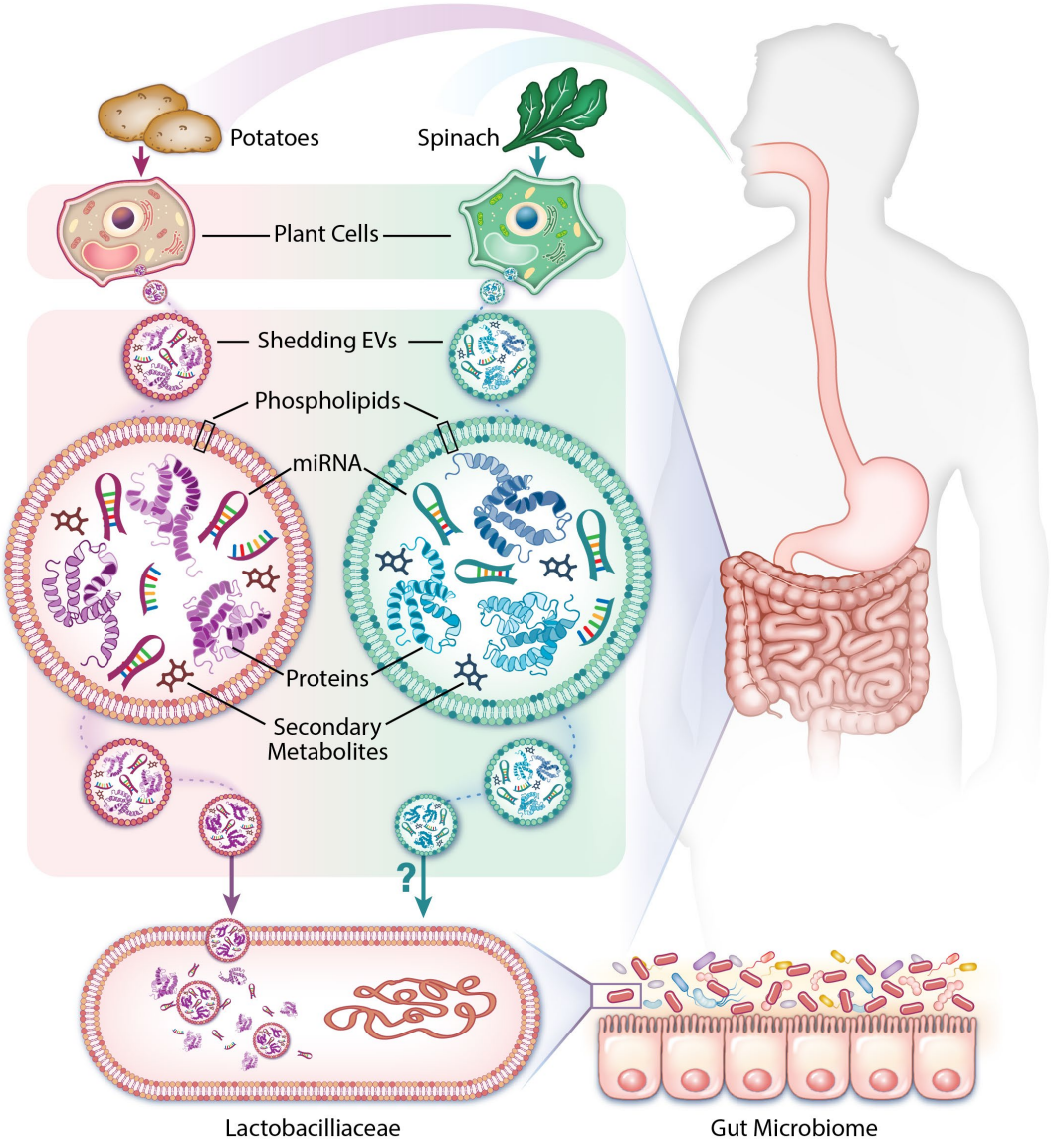

Figure 6. EPDEV-mediated communication from plant to bacteria and host. Plant-specific EVs are differentiated by phospholipid, protein, metabolite, and RNA content. Phospholipid content is thought to drive uptake by specific bacteria. Once internalized, EV-transported contents (protein, RNA, metabolites) has the potential to influence bacterial growth, gene expression, and metabolite production that could have downstream effects on gut health. Graphic image designed and generated by Karen Prince, Department of Pathology, Texas Children's Hospital.

Another interesting result found in this study was the recurring association of either potato-derived EVs or spinach-derived EVs with bacteria from the *Lachnospiraceae* family, the abundance of which is known to be influenced by diet. *Lachnospiraceae* are known to ferment diverse plant polysaccharides into important short-chain fatty acids like butyrate, which if produced in the colon improves the intestinal barrier, regulates intestinal motility,

and influences mucus production [53]. As reviewed in [54], a decreased abundance of *Lachnospiraceae* is associated with increased inflammation in the gut, specifically in GI diseases like irritable bowel syndrome and inflammatory bowel disease. Other consequences of having a gut microbiome low in butyrate producers include an increased risk for colonic infections, colorectal cancer and even extends to more systemic diseases like type 2 diabetes [54]. It is possible that EPDEVs positively influence the growth of specific butyrate producing bacteria, again supporting a hypothesis that gut microbes capable of specific health-benefits may have co-evolved synergistically to benefit host health through diet-mediated mechanisms that stem from plant-based diets rich in EPDEVs.

The size, concentration, and purity of plant EVs used in this study were comparable to those from previous research of potato EVs [55] and spinach EVs [56]. The composition and complexity of EPDEVs can vary based on factors like plant growth conditions, soil composition, watering practices, temperature, biotic stresses, and isolation protocols. These variables can cause daily fluctuations in the health benefits of these vesicles. Future studies will need to optimize crop growth conditions to maximize the health benefits of EPDEVs.

Preliminary analysis suggests that techniques like labeling, FACS, cell sorting, and sequencing can identify specific bacteria that take up plant EVs from mixed bacterial populations. This involves assessing the affinity of uptake and kinetic parameters, such as temperature dependency. For bacteria that can be cultured, further analysis could explore uptake preferences among specific microbes. Currently, EV populations are sourced directly from greenhouse plants, but future research will involve analyzing labeled EVs subjected to artificial digestion conditions.

Certainly, an area for future work is manipulating plant EVs to impact the gut microbiome and potentially impact human health [16,18,57–59]. These modifications could be to the EVs to control specificity of the microbial populations they interact with or to the content of the EVs to modulate microbial responses [2,3,60]. Some applications supported by *in vitro* studies include the targeted delivery of bioactive molecules like siRNA and anti-cancer drugs to suppress cancer cell growth [61,62]. Other applications of interest include the delivery of microRNAs that impact immune-regulation of inflammatory responses like MAPK and NF-κB signaling, increasing anti-inflammatory cytokine production, reducing pro-inflammatory cytokine secretion, T-cell activation, and macrophage polarization [62–65]. However, before these strategies can be effectively deployed it will be important that additional work be undertaken to access how plant growth conditions, packaging and cooking regimes impact plant EV bioactivity [66].The use of *in vitro* methods in this study provides valuable insights into the interactions between specific microbial communities and plant-derived EVs, generating hypothesis-driven data that can guide future research. These methods allow for a detailed investigation of microbial responses, which is essential for understanding the role of EVs in the gut microbiome. However, there are notable limitations. Replicating true dietary conditions is challenging, as the experimental setup does not account for interactions among different plant-derived EVs. Additionally, *in vitro* methods inherently cannot fully replicate *in vivo* conditions, and factors such as media composition and experimental design may limit the changes observed during microbial culturing. Despite

these limitations, the data obtained from these experiments are instrumental in expanding our understanding of microbial interactions with EVs and setting the stage for more comprehensive studies.

5. Conclusion

Recent studies on plant-derived EVs, including those presented here, offer new insights into how edible plants can impact human health. By examining the interactions between these vesicles and the gut microbiota, this research is transforming our understanding of the role of food in health. Extracellular vesicles from spinach, potatoes, and other crops show potential for both preventive and therapeutic applications due to their safety and ease of extraction. These vesicles can carry small-molecule drugs and nucleic acids, and their adaptable properties make them promising candidates for future research and applications.

Supplementary data

The authors confirm that the supplementary data are available within this article. Figure S1. Particle size distribution and concentration of potato-derived EVs. Figure S2. Potato-derived EVs influence the growth of lactobacilli. Figure S3. Particle size distribution and concentration of spinach-derived EVs.

Acknowledgements

We would like to acknowledge the Baylor College of Medicine SMART Program and SMART student Amanda Miller for her contributions to this project and Karen Prince of the Department of Pathology at Texas Children's Hospital for her graphic artistry. This work was supported by funds from the National Institute of Allergy and Infectious Diseases of the National Institutes of Health R03 AI149201 (K.H. & J.K.S) and the Collaborative Faculty Research Investment Program of The University of Houston and Baylor College of Medicine (K.H. & X.L.). Fluorescence Assisted Cell Sorting was performed by the Cytometry and Cell Sorting Core at Baylor College of Medicine with funding from the CPRIT Core Facility Support Award (CPRIT-RP180672), the NIH (P30 CA125123, S10 RR024574, and S10 OD025251) and the expert assistance of Joel M. Sederstrom.

Conflicts of interests

The authors declare there are no conflicts of interest to disclose.

Ethical statement

The donor stool was originally collected and the donor's health was screened under a study performed in accordance with the Declaration of Helsinki and approved by the Baylor College of Medicine Institutional Review Board (Protocol H-31066 approved 12/20/2012). At the time the material was deemed unusable, the stool was de-identified, labeled solely as

healthy human stool, and banked in a −80 freezer. An aliquot of this de-identified stool was utilized in this study.

Authors' contribution

Conceptualization, J.K.S. and K.H.; methodology, J.K.S., K.H., H.R., A.J.G., J.Y., M.A.E., J.K.R., R.A.L. and S.S.; data processing, A.V.S. and S.S.; formal analysis, J.K.S., K.H., and X.L.; investigation, J.K.S.; resources, J.K.S., K.H., and X.L.; data curation, J.K.S. and X.L.; writing—original draft preparation, J.K.S.; writing—review and editing, all authors; supervision, J.K.S., K.H., and X.L.; funding acquisition, J.K.S., K.H., and X.L. All authors have read and agreed to the published version of the manuscript.

References

[1] Tomova A, Bukovsky I, Rembert E, Yonas W, Alwarith J, *et al.* The Effects of Vegetarian and Vegan Diets on Gut Microbiota. *Front. Nutr.* 2019, 6:47.
[2] Kocholata M, Maly J, Martinec J,Auer Malinska H. Plant extracellular vesicles and their potential in human health research, the practical approach. *Physiol. Res.* 2022, 71(3):327–339.
[3] Kameli N, Dragojlovic-Kerkache A, Savelkoul P, Stassen FR. Plant-Derived Extracellular Vesicles: Current Findings, Challenges, and Future Applications. *Membranes (Basel)* 2021, 11(6):411.
[4] An Q, van Bel AJ, Huckelhoven R. Do plant cells secrete exosomes derived from multivesicular bodies? *Plant Signal. Behav.* 2007, 2(1):4–7.
[5] de la Canal L, Pinedo M. Extracellular vesicles: a missing component in plant cell wall remodeling. *J. Exp. Bot.* 2018, 69(20):4655–4658.
[6] Urzi O, Gasparro R, Ganji NR, Alessandro R,Raimondo S. Plant-RNA in Extracellular Vesicles: The Secret of Cross-Kingdom Communication. *Membranes (Basel)* 2022, 12(4):352.
[7] Regente M, Pinedo M, San Clemente H, Balliau T, Jamet E, *et al.* Plant extracellular vesicles are incorporated by a fungal pathogen and inhibit its growth. *J. Exp. Bot.* 2017, 68(20):5485–5495.
[8] Rutter BD, Innes RW. Extracellular vesicles as key mediators of plant-microbe interactions. *Curr. Opin. Plant Biol.* 2018, 44:16–22.
[9] Liu G, Kang G, Wang S, Huang Y ,Cai Q. Extracellular Vesicles: Emerging Players in Plant Defense Against Pathogens. *Front. Plant Sci.* 2021, 12:757925.
[10] De Palma M, Ambrosone A, Leone A, Del Gaudio P, Ruocco M, *et al.* Plant Roots Release Small Extracellular Vesicles with Antifungal Activity. *Plants (Basel)* 2020, 9(12):1777.
[11] Cui Y, Gao J, He Y, Jiang L. Plant extracellular vesicles. *Protoplasma* 2020, 257(1):3–12.
[12] Li Y, Zhang Q, Zhang J, Wu L, Qi Y, *et al.* Identification of microRNAs involved in pathogen-associated molecular pattern-triggered plant innate immunity. *Plant Physiol.* 2010, 152(4):2222–2231.
[13] Ding T, Li W, Li F, Ren M,Wang W. microRNAs: Key Regulators in Plant Responses to Abiotic and Biotic Stresses via Endogenous and Cross-Kingdom Mechanisms. *Int. J. Mol. Sci.* 2024, 25(2):1154.
[14] Miyamoto K, Kawase F, Imai T, Sezaki A, Shimokata H. Dietary diversity and healthy life expectancy-an international comparative study. *Eur. J. Clin. Nutr.* 2019, 73(3):395–400.

[15] Bukania ZN, Mwangi M, Karanja RM, Mutisya R, Kombe Y, *et al.* Food Insecurity and Not Dietary Diversity Is a Predictor of Nutrition Status in Children within Semiarid Agro-Ecological Zones in Eastern Kenya. *J. Nutr. Metab.* 2014, 2014:907153.
[16] Lian MQ, Chng WH, Liang J, Yeo HQ, Lee CK, *et al.* Plant-derived extracellular vesicles: Recent advancements and current challenges on their use for biomedical applications. *J. Extracell. Vesicles* 2022, 11(12):e12283.
[17] Teng Y, Ren Y, Sayed M, Hu X, Lei C, *et al.* Plant-Derived Exosomal MicroRNAs Shape the Gut Micobiota. *Cell Host Microbe* 2018, 24:1–16.
[18] Spinler JK, Oezguen N, Runge JK, Luna RA, Karri V, *et al.* Dietary impact of a plant-derived microRNA on the gut microbiome. *ExRNA* 2020, 2:11.
[19] Rutter BD, Rutter KL, Innes RW. Isolation and Quantification of Plant Extracellular Vesicles. *Bio. Protoc.* 2017, 7(17):e2533.
[20] Bhattacharjee S. DLS and zeta potential - What they are and what they are not? *J. Control. Release* 2016, 235:337–351.
[21] Sze A, Erickson D, Ren L,Li D. Zeta-potential measurement using the Smoluchowski equation and the slope of the current-time relationship in electroosmotic flow. *J. Colloid Interface Sci.* 2003, 261(2):402–410.
[22] Auchtung JM, Robinson CD, Britton RA. Cultivation of stable, reproducible microbial communities from different fecal donors using minibioreactor arrays (MBRAs). *Microbiome* 2015, 3:42.
[23] Engevik MA, Morra CN, Roth D, Engevik K, Spinler JK, *et al.* Microbial Metabolic Capacity for Intestinal Folate Production and Modulation of Host Folate Receptors. *Front. Microbiol.* 2019, 10:2305.
[24] Engevik MA, Luk B, Chang-Graham AL, Hall A, Herrmann B, *et al.* Bifidobacterium dentium Fortifies the Intestinal Mucus Layer via Autophagy and Calcium Signaling Pathways. *mBio* 2019, 10(3).
[25] Puzar Dominkus P, Stenovec M, Sitar S, Lasic E, Zorec R, *et al.* PKH26 labeling of extracellular vesicles: Characterization and cellular internalization of contaminating PKH26 nanoparticles. *Biochim. Biophys. Acta Biomembr.* 2018, 1860(6):1350–1361.
[26] Aagaard K, Petrosino J, Keitel W, Watson M, Katancik J, *et al.* The Human Microbiome Project strategy for comprehensive sampling of the human microbiome and why it matters. *FASEB J.* 2013, 27(3):1012–1022.
[27] Luna RA, Oezguen N, Balderas M, Venkatachalam A, Runge JK, *et al.* Distinct Microbiome-Neuroimmune Signatures Correlate With Functional Abdominal Pain in Children With Autism Spectrum Disorder. *Cell. Mol. Gastroenterol. Hepatol.* 2017, 3(2):218–230.
[28] Kozich JJ, Westcott SL, Baxter NT, Highlander SK, Schloss PD. Development of a dual-index sequencing strategy and curation pipeline for analyzing amplicon sequence data on the MiSeq Illumina sequencing platform. *Appl. Environ. Microbiol.* 2013, 79(17):5112–5120.
[29] Callahan BJ, McMurdie PJ, Rosen MJ, Han AW, Johnson AJ, *et al.* DADA2: High-resolution sample inference from Illumina amplicon data. *Nat. Methods* 2016, 13(7):581–583.
[30] Bokulich NA, Kaehler BD, Rideout JR, Dillon M, Bolyen E, *et al.* Optimizing taxonomic classification of marker-gene amplicon sequences with QIIME 2's q2-feature-classifier plugin. *Microbiome* 2018, 6(1):90.
[31] Robeson MS, II, O'Rourke DR, Kaehler BD, Ziemski M, Dillon MR, *et al.* RESCRIPt: Reproducible sequence taxonomy reference database management. *PLoS Comput. Biol.* 2021, 17(11):e1009581.

[32] Katoh K, Misawa K, Kuma K,Miyata T. MAFFT: a novel method for rapid multiple sequence alignment based on fast Fourier transform. *Nucleic Acids Res.* 2002, 30(14):3059–3066.
[33] Price MN, Dehal PS, Arkin AP. FastTree: computing large minimum evolution trees with profiles instead of a distance matrix. *Mol. Biol. Evol.* 2009, 26(7):1641–1650.
[34] Caporaso JG, Kuczynski J, Stombaugh J, Bittinger K, Bushman FD, *et al.* QIIME allows analysis of high-throughput community sequencing data. *Nat. Methods* 2010, 7(5):335–336.
[35] Parks DH, Tyson GW, Hugenholtz P,Beiko RG. STAMP: statistical analysis of taxonomic and functional profiles. *Bioinformatics* 2014, 30(21):3123–3124.
[36] Teng Y, Ren Y, Sayed M, Hu X, Lei C, *et al.* Plant-Derived Exosomal MicroRNAs Shape the Gut Microbiota. *Cell Host Microbe* 2018, 24(5):637–652 e638.
[37] Lee BH, Wu SC, Chien HY, Shen TL ,Hsu WH. Tomato-fruit-derived extracellular vesicles inhibit Fusobacterium nucleatum via lipid-mediated mechanism. *Food Funct.* 2023, 14(19):8942–8950.
[38] Wang X, Liu Y, Dong X, Duan T, Wang C, *et al.* peu-MIR2916-p3-enriched garlic exosomes ameliorate murine colitis by reshaping gut microbiota, especially by boosting the anti-colitic Bacteroides thetaiotaomicron. *Pharmacol. Res.* 2024, 200:107071.
[39] Sundaram K, Teng Y, Mu J, Xu Q, Xu F, *et al.* Outer Membrane Vesicles Released from Garlic Exosome-like Nanoparticles (GaELNs) Train Gut Bacteria that Reverses Type 2 Diabetes via the Gut-Brain Axis. *Small* 2024, 20(20):e2308680.
[40] Capurso L. Thirty Years of Lactobacillus rhamnosus GG: A Review. *J Clin. Gastroenterol.* 2019, 53:S1–S41.
[41] Snydman DR. The safety of probiotics. *Clin Infect Dis* 2008, 46(Suppl 2):S104–S111.
[42] Sindhu KN, Sowmyanarayanan TV, Paul A, Babji S, Ajjampur SS, *et al.* Immune response and intestinal permeability in children with acute gastroenteritis treated with Lactobacillus rhamnosus GG: a randomized, double-blind, placebo-controlled trial. *Clin. Infect. Dis.* 2014, 58(8):1107–1115.
[43] Guandalini S, Pensabene L, Zikri MA, Dias JA, Casali LG, *et al.* Lactobacillus GG administered in oral rehydration solution to children with acute diarrhea: a multicenter European trial. *J. Pediatr. Gastroenterol. Nutr.* 2000, 30(1):54–60.
[44] Majamaa H, Isolauri E, Saxelin M, Vesikari T. Lactic acid bacteria in the treatment of acute rotavirus gastroenteritis. *J. Pediatr. Gastroenterol. Nutr.* 1995, 20(3):333–338.
[45] Vanderhoof JA, Whitney DB, Antonson DL, Hanner TL, Lupo JV, *et al.* Lactobacillus GG in the prevention of antibiotic-associated diarrhea in children. *J. Pediatr.* 1999, 135(5):564–568.
[46] Korpela K, Salonen A, Virta LJ, Kumpu M, Kekkonen RA, *et al.* Lactobacillus rhamnosus GG Intake Modifies Preschool Children's Intestinal Microbiota, Alleviates Penicillin-Associated Changes, and Reduces Antibiotic Use. *PLoS One* 2016, 11(4):e0154012.
[47] Esposito C, Roberti A, Turra F, Cerulo M, Severino G, *et al.* Frequency of Antibiotic-Associated Diarrhea and Related Complications in Pediatric Patients Who Underwent Hypospadias Repair: a Comparative Study Using Probiotics vs Placebo. *Probiotics Antimicrob. Proteins* 2018, 10(2):323–328.
[48] Carucci L, Nocerino R, Paparo L, De Filippis F, Coppola S, *et al.* Therapeutic effects elicited by the probiotic Lacticaseibacillus rhamnosus GG in children with atopic dermatitis. The results of the ProPAD trial. *Pediatr. Allergy Immunol.* 2022, 33(8):e13836.
[49] Kalliomaki M, Salminen S, Arvilommi H, Kero P, Koskinen P, *et al.* Probiotics in primary prevention of atopic disease: a randomised placebo-controlled trial. *Lancet* 2001, 357(9262):1076–1079.

[50] Spinler JK, Sontakke A, Hollister EB, Venable SF, Oh PL, *et al.* From prediction to function using evolutionary genomics: human-specific ecotypes of Lactobacillus reuteri have diverse probiotic functions. *Genome Biol. Evol.* 2014, 6(7):1772–1789.
[51] Ambrosone A, Barbulova A, Cappetta E, Cillo F, De Palma M, *et al.* Plant Extracellular Vesicles: Current Landscape and Future Directions. *Plants (Basel)* 2023, 12(24):4141.
[52] He B, Hamby R, Jin H. Plant extracellular vesicles: Trojan horses of cross-kingdom warfare. *FASEB Bioadv.* 2021, 3(9):657–664.
[53] Vacca M, Celano G, Calabrese FM, Portincasa P, Gobbetti M, *et al.* The Controversial Role of Human Gut Lachnospiraceae. *Microorganisms* 2020, 8(4):573.
[54] Singh V, Lee G, Son H, Koh H, Kim ES, *et al.* Butyrate producers, "The Sentinel of Gut": Their intestinal significance with and beyond butyrate, and prospective use as microbial therapeutics. *Front. Microbiol.* 2022, 13:1103836.
[55] Lee Y, Jeong DY, Jeun YC, Choe H,Yang S. Preventive and ameliorative effects of potato exosomes on UVB-induced photodamage in keratinocyte HaCaT cells. *Mol. Med. Rep.* 2023, 28(3):167.
[56] Lee JH, Kang SJ, Rhee WJ. Exploiting Spinach-Derived Extracellular Vesicles for Anti-Obesity Therapy Through Lipid Accumulation Inhibition. *Adv. Ther.* 2024, 7(11):2400150.
[57] Hirschi K. Nutritional improvements in plants: time to bite on biofortified foods. *Trends Plant Sci.* 2008, 13(9):459–463.
[58] Nemati M, Singh B, Mir RA, Nemati M, Babaei A, *et al.* Plant-derived extracellular vesicles: a novel nanomedicine approach with advantages and challenges. *Cell Commun. Signal.* 2022, 20(1):69.
[59] Xu Z, Xu Y, Zhang K, Liu Y, Liang Q, *et al.* Plant-derived extracellular vesicles (PDEVs) in nanomedicine for human disease and therapeutic modalities. *J. Nanobiotechnol.* 2023, 21(1):114.
[60] Yang J, Primo C, Elbaz-Younes I,Hirschi KD. Bioavailability of transgenic microRNAs in genetically modified plants. *Genes Nutr.* 2017, 12:17.
[61] Li Z, Wang H, Yin H, Bennett C, Zhang HG, *et al.* Arrowtail RNA for Ligand Display on Ginger Exosome-like Nanovesicles to Systemic Deliver siRNA for Cancer Suppression. *Sci. Rep.* 2018, 8(1):14644.
[62] You JY, Kang SJ, Rhee WJ. Isolation of cabbage exosome-like nanovesicles and investigation of their biological activities in human cells. *Bioact. Mater.* 2021, 6(12):4321–4332.
[63] Han JM, Song HY, Lim ST, Kim KI, Seo HS, *et al.* Immunostimulatory Potential of Extracellular Vesicles Isolated from an Edible Plant, Petasites japonicus, via the Induction of Murine Dendritic Cell Maturation. *Int. J. Mol. Sci.* 2021, 22(19):10634.
[64] Wu J, Ma X, Lu Y, Zhang T, Du Z, *et al.* Edible Pueraria lobata-Derived Exosomes Promote M2 Macrophage Polarization. *Molecules* 2022, 27(23):8184.
[65] Raimondo S, Urzi O, Meraviglia S, Di Simone M, Corsale AM, *et al.* Anti-inflammatory properties of lemon-derived extracellular vesicles are achieved through the inhibition of ERK/NF-kappaB signalling pathways. *J. Cell. Mol. Med.* 2022, 26(15):4195–4209.
[66] Lo KJ, Wang MH, Ho CT,Pan MH. Plant-Derived Extracellular Vesicles: A New Revolutionization of Modern Healthy Diets and Biomedical Applications. *J. Agric. Food Chem.* 2024, 72(6):2853–2878.